


# P2X7R in Mast Cells is a Potential Target for Salicylic Acid and Aspirin in Treatment of Inflammatory Pain

Yucui Jiang<sup>1,2,\*</sup>Fan Ye<sup>1,\*</sup>Ying Du<sup>1</sup>Yingxin Zong<sup>1</sup>Zongxiang Tang<sup>1</sup> 

<sup>1</sup>School of Medicine & Holistic Integrative Medicine, Nanjing University of Chinese Medicine, Nanjing, Jiangsu, People's Republic of China; <sup>2</sup>School of Chinese Medicine & School of Integrated Chinese and Western Medicine, Nanjing University of Chinese Medicine, Nanjing, Jiangsu, People's Republic of China

\*These authors contributed equally to this work

**Background:** Mast cells are well known for their role in inflammatory pain. P2X7 receptor (P2X7R) has attracted much attention due to its prominent role in inflammatory diseases. Salicylates are commonly used anti-inflammatory and analgesic drugs. Until now, little has been known about whether P2X7R in mast cells is involved in inflammatory pain and whether it is a potential target for salicylates.

**Methods:** First, the expression of P2X receptors in mouse peritoneal mast cells was detected by using RT-PCR, immunofluorescence, calcium imaging and electrophysiological technique. In addition, the functions of P2X receptors, especially P2X7R, in mast cells were studied by using QPCR, ELISA and behavioral tests. Furthermore, P2X7R was used as a target to screen for some anti-inflammatory monomers that could inhibit its activity. At last, the effect of salicylic acid (SA) and aspirin (ASA) on the activity of P2X7R was studied by using calcium imaging, electrophysiological technique, ELISA, real-time PCR, behavioral tests, immunofluorescence and molecular docking.

**Results:** We found that P2X1, P2X3, P2X4 and P2X7 receptors were expressed in mouse peritoneal mast cells. The functions of different P2X receptors were various. Activation of P2X7R in mouse mast cells induced the release of inflammatory mediators, such as histamine, IL-1 $\beta$ , and CCL3. In addition, inflammation pain induced by high concentrations of ATP could be alleviated by P2X7R blockers or mast cell defects. Interestingly, SA or ASA could reduce high concentrations of ATP-induced inward current, P2X7R upregulation, mediators release, and inflammatory pain. SA or ASA also inhibited the inward current evoked by P2X7R agonist, BZATP. Molecular docking showed that SA or ASA had affinity for the cytoplasmic GDP-binding region of P2X7R.

**Conclusion:** P2X7R in mast cells was involved in inflammation pain by releasing inflammatory mediators, and P2X7R might be a potential target for SA and ASA analgesia.

**Keywords:** P2X7R, mast cells, salicylates, analgesia, inflammatory pain

## Introduction

Mast cells are in close proximity to afferents and establish dynamic interactions with pain-activating nociceptors.<sup>1</sup> Preformed and newly synthesized mediators released from mast cells, including proteoglycans, proteases, leukotrienes, biogenic amines, and cytokines, contribute to pain via nervous system or other immune cells. Therefore, mast cells play important roles in the pathological process of pain.<sup>2,3</sup> The classic pathway for mast cells activation is mediated by IgE receptor (Fc $\epsilon$ RI).<sup>4</sup> In addition, mast cells are also activated by a wide variety of triggers, such as substance P, lipid mediators, interleukins and extracellular ATP.<sup>5,6</sup>

Correspondence: Zongxiang Tang  
School of Medicine & Holistic Integrative Medicine, Nanjing University of Chinese Medicine, 138 Xianlin Avenue, Nanjing, Jiangsu Province  
Tel +86 25 85811802  
Email zongxiangtang@njutcm.edu.cn

Extracellular ATP is a “signal of danger” mediated by P2 purinergic receptors. P2 receptors have two types, P2X (P2X1-7) receptors and P2Y receptors.<sup>7</sup> P2X receptors carry out many important functions in the central and peripheral nervous system.<sup>8,9</sup> Compelling evidence has shown that P2X3, P2X4 and P2X7 receptors are involved in the pathogenesis of chronic pain.<sup>10</sup> P2X7R exists in neurons and glial cells of the nervous system, but is mainly expressed in cells of immune origin such as monocytes, macrophages, and microglia.<sup>11</sup> The absence of P2X7R can completely eliminate the inflammatory and neuropathic hypersensitivity to both mechanical and temperature stimulation.<sup>12–14</sup> P2X7R in microglia plays an important role in chronic neuropathy and inflammatory pain by releasing pro-inflammatory cytokines such as IL-1 $\beta$ .<sup>15</sup> Besides IL-1 $\beta$ , the production of cytokines such as IL-6, CCL2, TNF $\alpha$  and CCL3 are also mediated by P2X7R activation in microglia, neutrophil, and monocytes.<sup>16–20</sup> P2X7R is also expressed in a variety of mast cells, including LAD2, HMC-1, BMMCs, MC/9, and P815 mast cells.<sup>21</sup> Although activation of P2X4R can augment the degranulation mediated by Fc $\epsilon$ RI in mouse bone marrow-derived mast cells, only P2X7R activation contributes to degranulation in LAD2.<sup>22,23</sup> P2X7R in mast cells has also recently been proven to be crucial in inflammation diseases such as intestinal inflammation and meningeal neuroinflammation;<sup>24,25</sup> however, the relationship between P2X7R in mast cells and inflammation pain remains unclear.

Chronic pain is a global problem affecting more than two-thirds of the population. Extensive research has been conducted to find appropriate methods of relieving pain and improving the quality of life. The analgesics include opioids, nonopioid analgesics, and adjuvants or coanalgesics.<sup>26</sup> Salicylates are effective anti-inflammatory, analgesic, and antipyretic agents. Salicylic acid (SA), an extract of willow bark, was used for pain management as early as 4000 years ago. Aspirin (acetylsalicylic acid [ASA]) is the oldest and the most widely used analgesics in the world.<sup>27</sup> The main mechanism of action of salicylates is to inhibit the cyclooxygenase (COX) and prevent the formation of prostaglandins.<sup>28</sup> Although the analgesic effect of salicylates is obvious, the targets are still not entirely clear. Previous studies indicate that salicylates are associated with mast cells. SA can significantly inhibit histamine release from rat peritoneal mast cells activated by compound 48/80 or anti-DNP IgE.<sup>29</sup> The relationship between ASA and mast cells

remains controversial. Some evidence that shows the anaphylaxis triggered by ASA is due to eosinophils and mast cells.<sup>30</sup> Although Steinke et al reported that 10 mM ASA alone increased cysteinyl leukotrienes (CysLT) release, Mortaz et al have shown that that 10 mM ASA could inhibit IgE+Ag-mediated mast cells activation.<sup>31,32</sup> Little is known about the effects of SA or ASA on P2X7R in mast cells.

In the present study, we evaluated the roles of several P2X receptor subtypes in mouse mast cells, especially P2X7R. In addition, P2X7R was used as a target to screen for some anti-inflammatory monomers that inhibited the activity of P2X7R. Moreover, we also explored the effects of SA and ASA on P2X7R in mast cells.

## Materials and Methods

### Ethics Statement

All procedures were performed under protocols approved by the Animal Care and Use Committee of Nanjing University of Chinese Medicine (ACU190401). This research does not contain any studies with human participants performed by any of the authors.

### Animals

Adult male mice used were 22–26 g in a C57BL/6 background (Qinglongshan, China). Animals were housed at constant humidity (40–60%) and temperature (22  $\pm$  2  $^{\circ}$ C) on a 12 h light/dark cycle and allowed free access to food and water. C-kit mutant genetically mast cell-deficient Kit (W-sh) “Sash” mice and Mrgprb2-Cre tdT +mice were donated by Johns Hopkins.

### Chemicals

We used the following chemicals: ATP disodium salt (Sigma-Aldrich, St. Louis, MO, United States), PPADS (20  $\mu$ M, Abcam, USA, a non-selective P2 purinergic receptor antagonist), NF449 (1  $\mu$ M, Cayman, USA, P2X1R antagonist), AF-353 (0.1  $\mu$ M, donated by China Pharmaceutical University, P2X3R antagonist), 5-BDBD (10  $\mu$ M, Sigma-Aldrich, United States, P2X4R antagonist), AZ10606120 (1  $\mu$ M, Tocris Bioscience, USA, P2X7R antagonist), BzATP (30  $\mu$ M, Alomone Labs, Israel, P2X7R agonist), recombinant mouse SCF protein (10 ng/mL, R&D Systems, USA), penicillin and streptomycin (100  $\mu$ g/mL; Gibco, USA), fibronectin (30  $\mu$ g/mL; Sigma-Aldrich, United States), Fluo 4-AM (Solarbio, China, calcium indicator), Histamine ELISA Kit

(Yifeixue, China), IL-1 $\beta$  ELISA Kit (Yifeixue, China), Trizol (Vazyme Biotech, China), HiScript II Q RT SuperMix for qPCR (Vazyme Biotech, China), Taq MasterMix (Vazyme Biotech, China), AceQ qPCR SYBR Green Master Mix (Vazyme Biotech, China), ATP Content Assay Kit (Yifeixue, China), salicylic acid (Yuanye Biotech, China), aspirin (Yuanye Biotech, China), Rabbit Anti-P2RX7 antibody (Bioss, China)

## P815 Cells Culture and Mouse Peritoneal Mast Cell Purification

Mouse mastocytoma cells (P815) were purchased from the Shanghai Institute of Biochemistry and Cell Biology. P815 was cultured in 1640 complete medium (90% 1640 medium, 10% fetal bovine serum, 100  $\mu$ g/ mL penicillin and 100  $\mu$ g/ mL streptomycin). Cells were incubated in an incubator humidified with 5% CO<sub>2</sub> at 37 °C.

Mouse peritoneal mast cells were obtained from C57BL/6 mice as Dong's Lab described.<sup>33</sup> Briefly, the mouse peritoneal cells were collected by mast cell dissociation media MCDM (HBSS with 10 mM HEPES and 3% fetal bovine serum, PH was 7.2) and centrifuged at 200 g for 5 min. The pellet was resuspended and layered over 70% percoll suspension, and then centrifuged at 500 g at 4°C for 20 min. The supernatant was carefully sucked

away by pipette and the mast cells were washed with fresh MCDM. Mast cells were resuspended in DMEM containing 10% fetal bovine serum and 10 ng/mL recombinant mouse SCF. As [Supplementary Figure S1](#) showed, the isolated mouse peritoneal mast cells were identified by toluidine blue staining and the purity was about 90%.

## P2X Purinoceptors RT-PCR Screen

The TRIzol<sup>®</sup> method was used to isolate total RNA from mouse peritoneal mast cells or the P815 cells. We used 10–500 ng RNA for reverse transcription reaction by using HiScript II Q RT SuperMix for qPCR Kit according to the manufacturer's instructions. Polymerase chain reaction conditions were as follows: 95 °C for 5 min, 40 cycles of 15 s at 95 °C, 30 s at 60°C (56 °C for P2X4R), 1 min at 72 °C, and 10 min at 72 °C. The PCR primers were synthesized by GenScript Biotech (Nanjing, China). The primer sequences and product sizes are shown in [Table 1](#).

## Intracellular Calcium Measurement

Mouse peritoneal mast cells were isolated and placed on slides coated with 30  $\mu$ g/ mL fibronectin. After 2 h of culture, mast cells were incubated with 1  $\mu$ L/mL Fluo-4 and 0.02% Pluronic F-127 at room temperature for 30 min. The cells then immediately washed 3 times by calcium

**Table 1** The Sequence of Primers and the Size of PCR product

Gene	Primer Sequence (5'-3')	Product Size
P2X1	Forward: GCCCAAGGTATTCGCACAGG	496 bp
	Reverse: GACGACGGTTTGTCCCATTCT	
P2X2	Forward: ACCTGCCATTTAGATGACGACTG	241 bp
	Reverse: TGTTGCCCTTGGAGAACTTGA	
P2X3	Forward: GCTTCGGACGCTATGCCAACA	490 bp
	Reverse: AAATCCTGCCAGCAAACCTTAA	
P2X4	Forward: GTGCTCGGGTCCTTCTGTTC	154 bp
	Reverse: CCGTTTCCTGGTAGCCCTTTT	
P2X5	Forward: TGTAGCGGGACACGGACTGA	209 bp
	Reverse: TTTCTAGCACATTGGCTTTGGA	
P2X6	Forward: GGTACAACCTCAGGACAGCCAATC	207 bp
	Reverse: CACACAGTAGCAGCAGGTCACAGAG	
P2X7	Forward: AACATCTTGCCAACTATGAACGG	132 bp
	Reverse: TCCTCCCTGAACTGCCACCT	

imaging buffer (125 mM NaCl, 3 mM KCl, 2.5 mM CaCl<sub>2</sub>, 0.6 mM MgCl<sub>2</sub>, 20 mM glucose, 10 mM HEPES, 20 mM sucrose, 1.2 mM NaHCO<sub>3</sub>, PH was 7.4). Finally, the cells were imaged at 488-nm excitation to detect intracellular calcium within two hours. Each experiment was done at least three times, and at least 200 cells were analyzed each time.

## Whole-Cell Current-Clamp Recordings of Mouse Peritoneal Mast Cells

All the experiments were performed at room temperature. Whole-cell currents were recorded by using Multiclamp 700 B and Digidata 1440 A (Molecular Devices, Inc., San Jose, USA). Experiments were performed with a perfusion system, and drugs were directly added to the recording chamber with a pipette. The cells were usually evoked by holding the membrane potential, and applied voltage commands to a range of potentials with 10 mV steps from -130 mV to +130 mV duration 100 ms. In addition, currents were evoked by ramping the membrane potential from -90 mV to +100 mV duration for 300 ms. The currents were digitized (sampled at a frequency of 10 kHz and filtered at 0.1 kHz for analysis), stored and subsequently analyzed by using Clampex 10.3 (Molecular Devices, Inc., San Jose, USA). The electrode resistance was 4–6 MΩ, and the osmolality of the pipette solution and external solution was adjusted to 300–310 mOsm (adjusted by sucrose as necessary). The standard pipette solution contained 135 mM CsCl, 8 mM NaCl, 10 mM EGTA, 3.6 mM CaCl<sub>2</sub>, 10 mM HEPES, 2 mM Mg-ATP (added when detecting P2X7 channel), PH was 7.3 (adjusted by CsOH). The standard external solution contained 147 mM NaCl, 2 mM KCl, 2 mM CaCl<sub>2</sub>, 1 mM MgCl<sub>2</sub>.6H<sub>2</sub>O, 10 mM HEPES, 16 mM glucose, PH was 7.3 (adjusted by NaOH). Low divalent external solution contained 147 mM NaCl, 10 mM HEPES, 13 mM glucose, 0.2 mM CaCl<sub>2</sub>, 2 mM KCl, PH was 7.3 (adjusted by NaOH).

## Quantitative Real-Time PCR

P815 Cells (about 10<sup>5</sup>–10<sup>6</sup> cells) were stimulated by different concentrations of ATP for 0.5, 4, or 8 hours and the paw tissues (10–50 mg) were treated with 100 mM ATP for 1 hour and were collected. Total RNA was extracted by using the TRIzol method. cDNA was generated by using HiScript II Q RT SuperMix for qPCR Kit according to the

manufacturer's instruction. Real-time qPCR was performed by using AceQ qPCR SYBR Green Master Mix and GAPDH were used as the internal controls. The primer sequences are shown in Table 2.

## ATP Measurement

ATP was measured by using ATP Content Assay Kit (Yifeixue, China). The principle of ATP content determination is that hexokinase catalyzes glucose and ATP to synthesize glucose-6-phosphate, and glucose-6-phosphate dehydrogenase further catalyzes dehydrogenation of glucose-6-phosphate to form NADPH. NADPH has a characteristic absorption peak at 340nm, which is proportional to the ATP content. We conducted the experiment according to the manufacturer's instruction. The paw tissue (about 10 mg) were homogenized and centrifuged at 8000g at 4°C for 10 min, and the supernatant was collected. After chloroform treatment, the supernatant was collected to detect ATP content.

## ELISA

The concentrations of histamine, CCL3 and IL-1β were determined by ELISA kit (Yifeixue, China). The assay was performed according to the manufacturer's protocol. In brief, mouse peritoneal mast cells were stimulated with different concentrations of ATP. Supernatant was collected after ATP stimulation for 0.5 h and stored at 80 °C for histamine detection. The supernatants of P815 cells in control group, ATP group, SA treatment group (500 μM, pretreatment for 2 h) and

**Table 2** The Sequence of Primers

Gene	Primer Sequence (5'-3')
IL-6	Forward: GTTGCCTTCTTGGGACTGAT
	Reverse: CTGGCTTTGTCTTTCTTGTAT
IL-1β	Forward: AAATCTCGCAGCAGCACATC
	Reverse: AGCAGGTTATCATCATCATCCC
CCL2	Forward: GGCCTGCTGTTACAGTTGC
	Reverse: CAGAAGTGCTTGAGGTGGTTG
CCL3	Forward: GCTCCAGCCAGGTGTCATT
	Reverse: CAGGCATTAGTTCCAGGTCAG
GAPDH	Forward: GCACAGTCAAGGCCGAGAAT
	Reverse: GCCTTCTCCATGGTGGTGAA

ASA treatment group (1 mM, pretreatment for 2 h) was collected and stored at 80 °C for CCL3 and IL-1 $\beta$  detection.

## Pain Model

Complete Freund's adjuvant (CFA) was injected unilaterally into the plantar surface of one hindpaw in mice (20  $\mu$ L), whereas control mice were injected with 0.9% saline. On the 5th day after CFA injection, the tissue of hindpaw was collected and the ATP content was detected.

## Behavioral Assays

The von Frey behavioral assays were performed in a blinded manner. In brief, different groups of mice were put in a transparent plastic box, which was placed on a metal mesh for about 30 min. Each mouse was tested more than 5 times at a specific force manually, and the threshold was determined by the lowest force needed to elicit responses more than 50% of the times. The mechanical threshold was measured at 1 h, 3 h and 5 h after ATP treatment (100 mM, PH was 7.32, 10  $\mu$ L, intradermal injection), respectively. Each mouse was manually tested at a specific force (0.16 g) at least 10 times.

## Histological Assays

The paw tissue treated with 100 mM ATP for 1 hour was isolated and fixed with 4% paraformaldehyde for 24 h and 30% sucrose for 48 h. The tissue was embedded in OCT and sliced to a thickness of 10 microns, followed by hematoxylin-eosin (HE) staining. Images of each section were obtained by using the Nikon ECLIPSE 80i microscope (Nikon, Tokyo, Japan) with a magnification of 250.

## Immunofluorescence Staining

OCT-embedded paw tissue sections, mouse peritoneal mast cells or P815 cells were fixed by 4% paraformaldehyde for 10 minutes. After washing 3 times with PBS, sections or P815 cells were blocked with 3% BSA and incubated in primary antibody solution overnight at 4 °C. After washing 3 times with PBS, sections or P815 cells were incubated with iFluor 488 or 555 goat anti-rabbit IgG for 1 hour at 37 °C. Mouse peritoneal mast cells or P815 cells were washed and mounted. The tissue sections were washed and incubated with FITC-avidin for 0.5 hour. Next, sections were washed and mounted in Prolong Gold Antifade Reagent with DAPI. At last, sections were evaluated on Nikon ECLIPSE 80i microscope with a magnification of 250.

## Molecular Docking

The discovery Studio 2016 4.0 software was used to verify the molecular docking. We downloaded the three-dimensional structure of salicylic acid (PubChem CID: 338) and aspirin (PubChem CID: 2244) from the NCBI PubChem Compound database (<http://www.ncbi.nlm.nih.gov/pccompound>) and the monomeric crystal structure of P2X7R (PDB ID: 6U9V) from the Research Collaboratory for Structural Bioinformatics (RCSB) Protein Data Bank (<http://www.rcsb.org/pdb>).

## Quantification and Statistical Analysis

The data were analyzed by GraphPad 8.0 and presented as mean  $\pm$  SEM. Statistical analysis of the results was performed by two-tailed, unpaired or paired Student's *t*-test, or one-way ANOVA analysis for comparing all pairs of groups.

## Results

### P2X Receptors Expression and ATP-Induced Calcium Response in Mouse Peritoneal Mast Cells

Extracellular ATP has been reported to increase during tissue stress, hypoxia, or inflammation. Our results showed that ATP was significantly increased in inflammatory pain induced by Complete Freund's adjuvant ([Supplementary Figure S2](#)), which may be due to the release of ATP by infiltrating inflammatory cells. In addition, mast cells are known to play important roles in inflammatory pain. Therefore, we suggest that mast cells may be involved in inflammatory pain through the purinergic signaling pathway.

First of all, we explored P2X receptors expression in mouse peritoneal mast cells by using RT-PCR. As shown in [Figure 1A](#), we found that mouse peritoneal mast cells expressed several P2X receptors including P2X1R, P2X3R, P2X4R and P2X7R. P2X receptors are a non-selective cation channel, and its permeability to Ca<sup>2+</sup> is the most obvious. Hence, we examined calcium influx induced by ATP in mouse peritoneal mast cells. The results showed that calcium influx in mast cells increased immediately after treatment with ATP ([Figure 1B and C](#)). The fluorescence intensity ratio varied with the ATP concentration and the EC50 was about 6.5  $\mu$ M ([Figure 1C](#)). In addition to fluorescence intensity, the reaction durations also had differences ([Figure 1B](#), bottom), indicating that different concentrations of ATP activate mast cells through different P2X receptors.

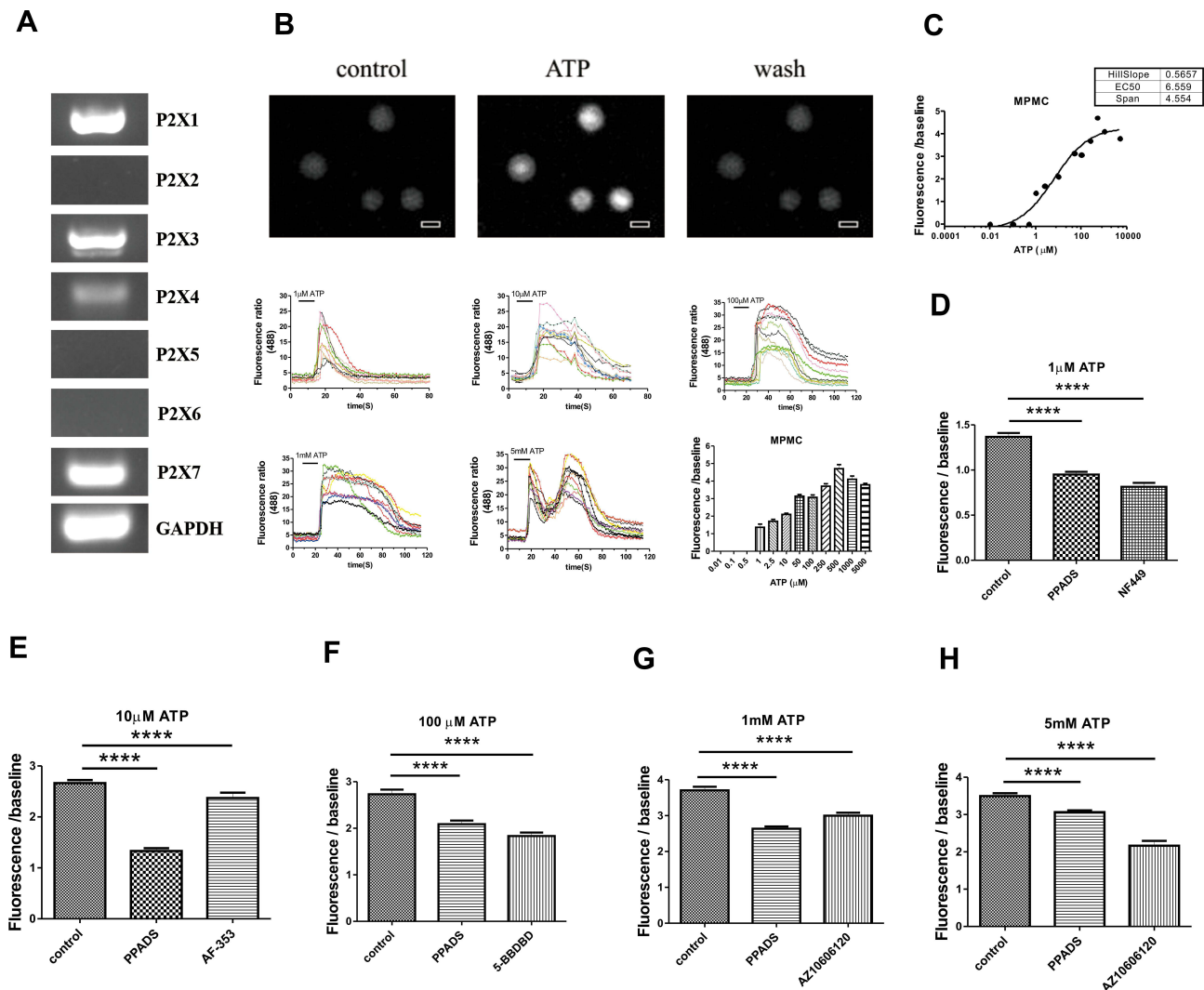


**Figure 1** P2X receptors expression and ATP-induced calcium response in mouse peritoneal mast cells. **(A)** P2X1R, P2X3R, P2X4R and P2X7R expressed in mouse peritoneal mast cells. **(B)** Heat map of  $[Ca^{2+}]_i$  (top) and example traces (bottom) mediated by different concentrations of extracellular ATP (Scal bar=10  $\mu$ m). **(C)** The fluorescence intensity of  $Ca^{2+}$  induced by different concentrations of ATP from 0.01 to 5000  $\mu$ M, and the EC50 was about 6.5  $\mu$ M. **(D)** Calcium influx induced by 1  $\mu$ M ATP was inhibited by PPADS or NF449 ( $****p < 0.0001$ , control vs PPADS or NF449). **(E)** Calcium influx induced by 10  $\mu$ M ATP was blocked by PPADS or AF-353 ( $****p < 0.0001$ , control vs PPADS or AF-353). **(F)** Calcium influx induced by 100  $\mu$ M ATP was blocked by PPADS or 5-BDBD ( $****p < 0.0001$ , control vs PPADS or 5-BDBD). **(G)** Calcium influx induced by 1 mM ATP was blocked by PPADS or AZ10606120 ( $****p < 0.0001$ , control vs PPADS or AZ10606120). **(H)** Calcium influx induced by 5 mM ATP was blocked by PPADS or AZ10606120 ( $****p < 0.0001$ , control vs PPADS or AZ10606120). (Statistical analysis of the results was performed by one-way ANOVA analysis followed by Dunn's multiple comparisons test).

To confirm this, we used special P2X channel antagonists. As shown in **Figure 1D–H**, calcium influx caused by ATP at different concentrations could be partially blocked by non-selective P2 purinergic receptor antagonist PPADS (20  $\mu$ M, pre-incubation for 5 minutes). In addition, calcium influx caused by 1  $\mu$ M ATP was inhibited by P2X1R antagonist NF449 (1  $\mu$ M, pre-incubation for 5 minutes) (**Figure 1D**). AF-353 (P2X3R antagonist, 0.1  $\mu$ M, pre-incubation for 5 minutes) reduced the calcium influx caused by 10  $\mu$ M ATP (**Figure 1E**). And the transient increase of intracellular calcium induced by 100  $\mu$ M ATP was blocked by 5-BDBD (10  $\mu$ M, pre-incubation for 5 minutes, P2X4R antagonist) (**Figure 1F**).

In addition, the specific P2X7R antagonist AZ10606120 (1  $\mu$ M, pre-incubation for 5 min) could block calcium influx caused by high concentrations of ATP such as 1 mM and 5 mM (**Figure 1G and H**). These results suggested that P2X1R, P2X3R, P2X4R and P2X7R might be involved in the activation of mast cells.

### Different Inward Currents Evoked by Extracellular ATP in Mouse Peritoneal Mast Cells

According to published literature, human mast cells are sensitive to ATP in a concentration-dependent manner.<sup>6</sup>

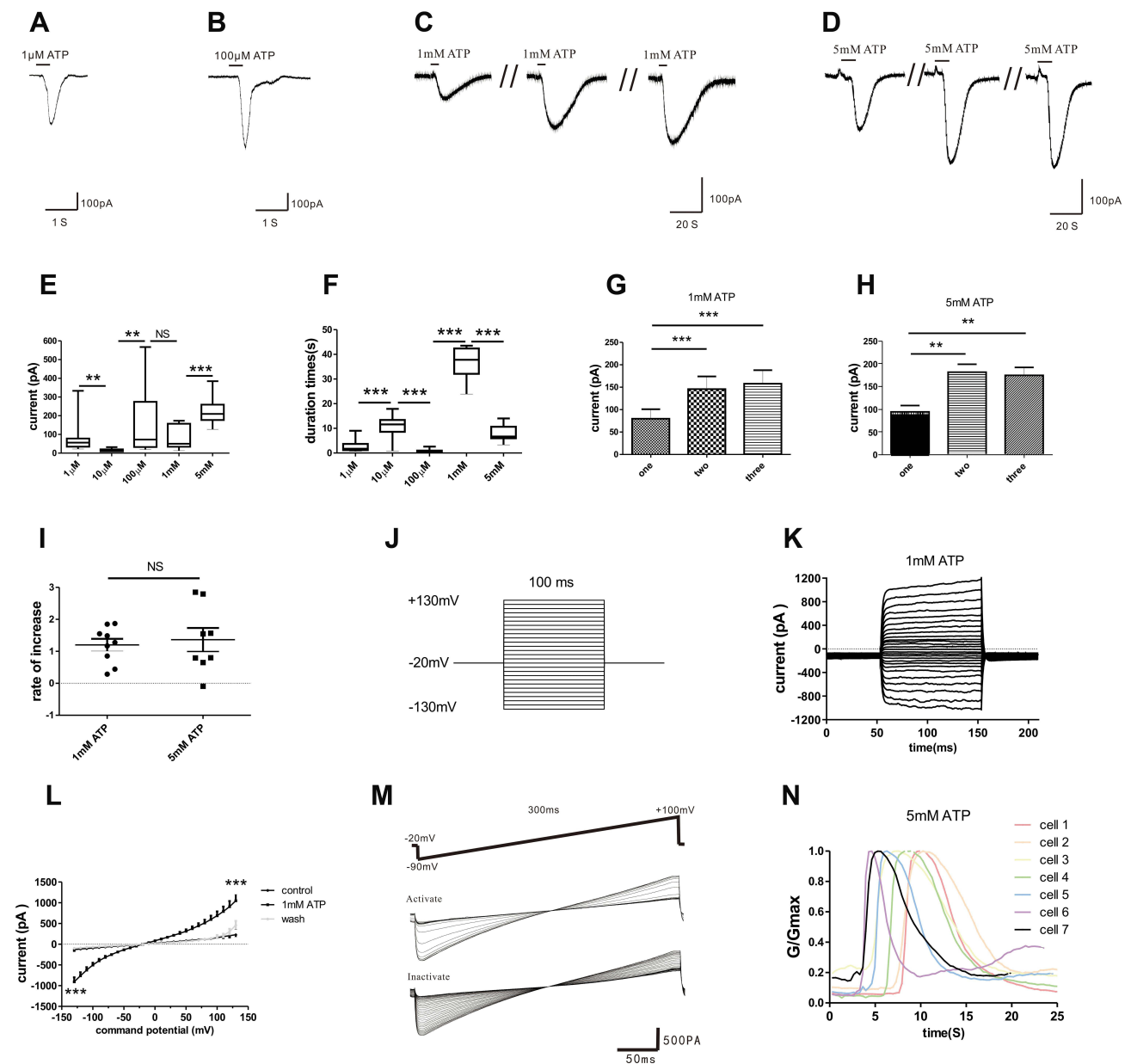


**Figure 2** Characteristics of inward currents in mouse peritoneal mast cells evoked by different concentrations of ATP. (A–D) Different currents induced by various concentrations of ATP (1  $\mu$ M, 100  $\mu$ M, 1 mM and 5 mM ATP respectively). (E) The current amplitude induced by various concentrations of extracellular ATP was different (\*\* $p < 0.01$ , 1  $\mu$ M vs 10  $\mu$ M, \*\* $p < 0.01$ , 10  $\mu$ M vs 100  $\mu$ M, \*\*\* $p < 0.001$ , 1 mM vs 5 mM, one-way ANOVA analysis followed by Dunnett's multiple comparisons test). (F) The duration of inward currents evoked by different concentrations of extracellular ATP was different (\*\*\* $p < 0.001$ , 1  $\mu$ M vs 10  $\mu$ M, 10  $\mu$ M vs 100  $\mu$ M, 100  $\mu$ M vs 1 mM, 1 mM vs 5 mM, one-way ANOVA analysis followed by Dunnett's multiple comparisons test). (G and H) The “run-up” tendency of inward currents induced by 1 mM ATP and 5 mM ATP. (I) No significant changes in the growth rate between 1 mM ATP- and 5 mM ATP-induced currents. (J) Stimulation protocol. (K) The different currents under this protocol stimulation. (L) The relationship curve of voltage-current. (M) The activate curves and inactivate curves induced by 5 mM ATP. (N) The conductance curve induced by 5 mM ATP.

Our experimental results proved that mouse peritoneal mast cells had the same properties. 1  $\mu$ M ATP (Figure 2A,  $n=17$ ) and 100  $\mu$ M ATP could induce obvious inward currents in mouse peritoneal mast cells (Figure 2B,  $n=21$ ). When we increased the concentration of extracellular ATP to a higher level, we found that both 1 mM ATP and 5 mM ATP had the ability to repeatedly induce inward currents (Figure 2C,  $n=9$ ;

Figure 2D,  $n=8$ ). As Figure 2E and F showed, the characteristics of the currents induced by different concentrations of ATP were different, including the amplitude and duration of the inward currents. Despite the differences, the inward currents evoked by 1 mM ATP and 5 mM ATP had some similar characteristics, such as “run-up” tendency (Figure 2G and H). There was no difference in the current

growth rate between 1 mM ATP-induced current and 5 mM ATP-induced current, as shown in [Figure 2I](#). The current growth rate is defined as the second current amplitude minus the first current amplitude divided by the first current amplitude. In addition, the inward current evoked by 1 mM ATP was voltage-dependent ([Figure 2J–L](#)). Furthermore, the activation curve and inactivation curve induced by 5 mM ATP were shown in [Figure 2M](#). The conductance curves that obtained from these curves were shown in [Figure 2N](#), indicating that the current induced by 5 mM ATP was characterized by fast activation and slow deactivation.

## P2X1R, P2X3R, P2X4R and P2X7R Were Expressed in Mouse Peritoneal Mast Cells

The above results indicate that different concentrations of ATP corresponded to different currents. Therefore, we hypothesized that multiple P2X receptors were involved in the activation progresses. In our study, we found that 1  $\mu$ M ATP hardly induced inward current when 20  $\mu$ M PPADS (a non-selective P2 antagonist) ([Figure 3A and G](#),  $n=9$ ) or 1  $\mu$ M NF449 (the blocker of P2X1R) ([Figure 3A and G](#),  $n=13$ ) was applied, which indicated that P2X1R was activated by 1  $\mu$ M ATP. As [Figure 3B and H](#) showed, 20  $\mu$ M PPADS ( $n=9$ ) or 0.1  $\mu$ M AF-353 (the blocker of P2X3 receptor,  $n=10$ ) could inhibit the current evoked by 10  $\mu$ M ATP, indicating that P2X3R was activated by 10  $\mu$ M ATP. We also found that P2X4R was involved in the current induced by 100  $\mu$ M ATP, which was blocked by 10  $\mu$ M 5-BDBD ([Figure 3C and I](#),  $n=10$ ) or 20  $\mu$ M PPADS ([Figure 3C and I](#),  $n=13$ ). The current caused by 1 mM ATP were inhibited by using 1  $\mu$ M AZ 10606120 (the blocker of P2X7 receptor) ([Figure 3D and J](#),  $n=5$ ). The current evoked by 5 mM ATP could also be blocked by 1  $\mu$ M AZ 10606120 ([Figure 3E and K](#),  $n=6$ ). This indicated that P2X7R could be activated by high concentrations of ATP. Interestingly, we found that 20  $\mu$ M PPADS could partially inhibit the current induced by 1 mM ATP ([Supplementary Figure S3A, S3C](#)), but had no effect on the current evoked by 5 mM ATP ([Supplementary Figure S3B, S3D](#)), which indicated that PPADS might have limited inhibitory effect on the activity of P2X7R. In addition, P2X7R was reported to be sensitive to divalent cations.<sup>34</sup> Our results also showed that in the low divalent cationic external solution, the inward current induced by 5 mM ATP was greater than that of the normal external solution ([Figure 3F and L](#)), which confirmed the presence of P2X7R in mouse peritoneal mast cells. Furthermore, the

presence of P2X7R was further confirmed by immunofluorescence ([Figure 3M–O](#)). Taken together, our results illustrated that P2X1R, P2X3R, P2X4R and P2X7R were expressed in mouse peritoneal mast cells and were involved in the activation induced by extracellular ATP.

## Activation of P2X7R in Mouse-Derived Mast Cells Induced Cytokines Synthesis

Degranulation is one of important indicators of mast cell activation. Consistent with the research of Wareham et al<sup>6</sup>, our results showed that there is no detectable histamine release at lower concentrations of ATP, such as 1  $\mu$ M and 100  $\mu$ M; however, histamine released from mouse peritoneal mast cells was significantly increased at higher concentrations of ATP ([Figure 4A](#)). In addition to histamine, mast cells are effective producers of inflammatory cytokines in response to various stimuli. The regulation of extracellular ATP on cytokine synthesis in mast cells remains unclear. Therefore, we detected the synthesis of a series of mediators such as IL-6, IL-1 $\beta$ , CCL2 and CCL3. The mouse peritoneal mast cells were too few to be detected, so we used P815 cells instead. P815 cells also expressed P2X1R, P2X3R, P2X4R, and P2X7R ([Supplementary Figure S4, Figure 4B](#)). [Figure 4C–G](#) showed the regulation of mediator synthesis was also related to ATP concentration. There was no significant change in the expression of cytokines in P815 cells stimulated with low concentrations of ATP (PH was 7.32, adjusted by NaOH) ([Figure 4C–E](#)). ATP with high concentrations (PH was 7.32, adjusted by NaOH) could significantly up-regulate the expression of cytokines, including IL-1 $\beta$  and CCL3 ([Figure 4F and G](#)). AZ10606120, a specific P2X7R antagonist (5  $\mu$ M, pre-incubation for 5 minutes), almost completely blocked the upregulation of IL-1 $\beta$  and CCL3 induced by 5 mM ATP ([Figure 4H](#)). Therefore, we believed that P2X7R in mast cells could mediate mast cells degranulation and de novo synthesis of inflammatory factors such as IL-1 $\beta$  and CCL3.

## High Concentrations of ATP Induced Inflammation Pain by Activating P2X7R in Mast Cells

Activation of P2X7R in mast cells modulates the synthesis of inflammatory mediators that may further cause pain through neuro-immune interactions. We assumed that mast cells and P2X7R promoted the inflammatory



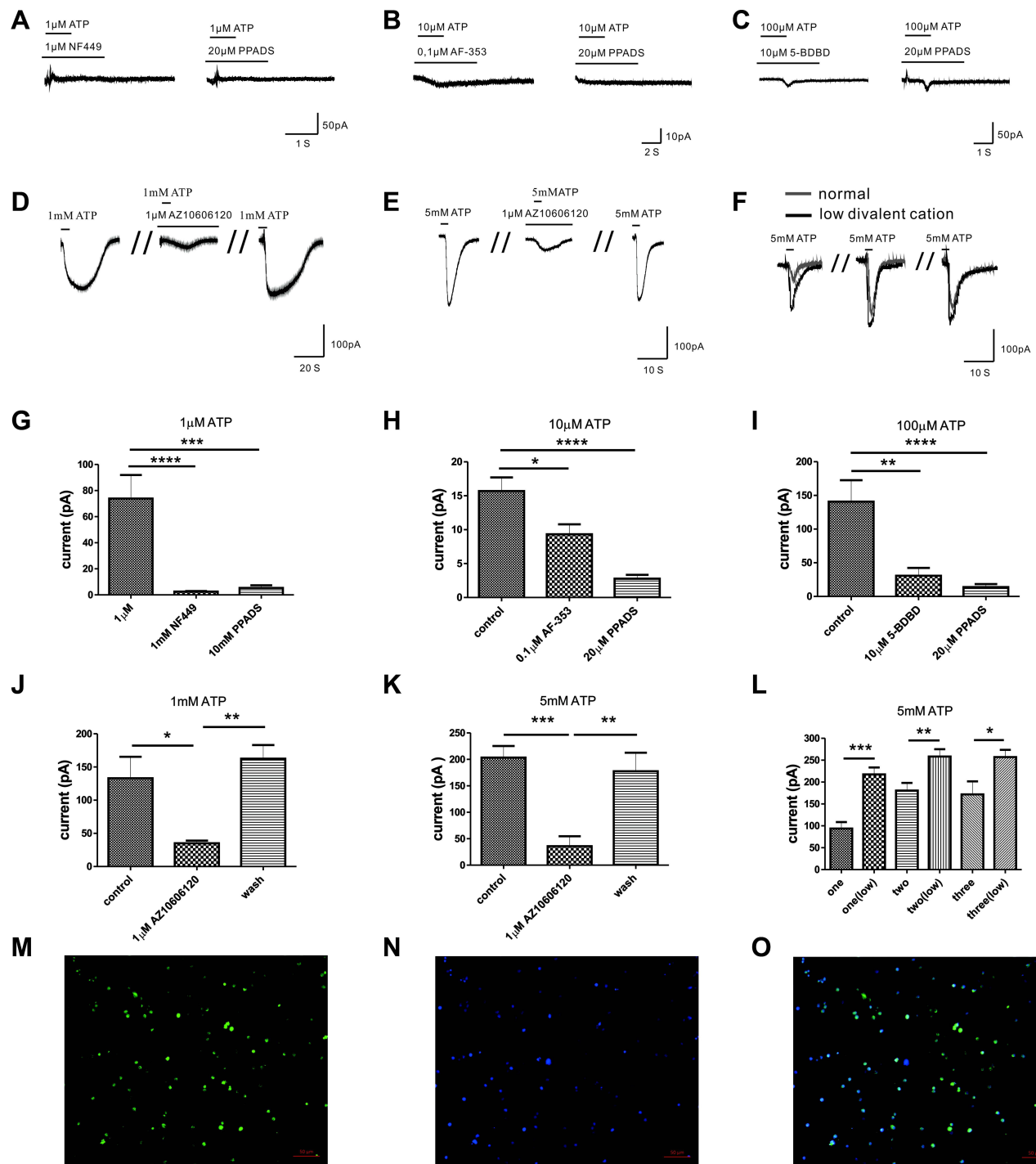


**Figure 3** The effects of specific blockers on the currents evoked by extracellular ATP. **(A)** Cell with 20  $\mu$ M PPADS or 1  $\mu$ M NF449 hardly evoke current by 1  $\mu$ M ATP treatment. **(B)** Current evoked by 10  $\mu$ M ATP could be blocked by 20  $\mu$ M PPADS or 0.1  $\mu$ M AF-353. **(C)** The current induced by 100  $\mu$ M ATP could be inhibited by 20  $\mu$ M PPADS or 10  $\mu$ M 5-BDBD. **(D)** The current induced by 1 mM ATP could be blocked by 1  $\mu$ M AZ10606120. **(E)** 1  $\mu$ M AZ10606120 could reduce the current evoked by 5 mM ATP. **(F)** 5 mM ATP could evoke greater inward current in the external solution with low divalent cation. **(G)** The current amplitude induced by 1  $\mu$ M ATP could be inhibited by PPADS or NF449 (\*\*\*\* $p$  < 0.0001, control vs 20  $\mu$ M PPADS,  $n=9$ , \*\*\*\* $p$  < 0.0001, control vs 1  $\mu$ M NF449,  $n=13$ , one-way ANOVA analysis followed by Dunnett's multiple comparisons test). **(H)** The current amplitude evoked by 10  $\mu$ M ATP was blocked by PPADS or AF-353 (\*\*\*\* $p$  < 0.0001, control vs 20  $\mu$ M PPADS,  $n=9$ , \* $p$  < 0.05, control vs 0.1  $\mu$ M AF-353,  $n=10$ , one-way ANOVA analysis followed by Dunnett's multiple comparisons test). **(I)** PPADS or 5-BDBD could inhibit the current amplitude evoked by 100  $\mu$ M ATP (\*\* $p$  < 0.01, control vs 20  $\mu$ M PPADS,  $n=13$ , \*\*\*\* $p$  < 0.0001, control vs 10  $\mu$ M 5-BDBD,  $n=10$ , one-way ANOVA analysis followed by Dunnett's multiple comparisons test). **(J)** The current amplitude evoked by 1 mM ATP was blocked by AZ10606120 (\* $p$  < 0.05, control vs 1  $\mu$ M AZ10606120,  $n=5$ , paired Student's  $t$ -test). **(K)** The current amplitude evoked by 5 mM ATP could also be blocked by AZ10606120 (\*\*\* $p$  < 0.001, control vs 1  $\mu$ M AZ10606120,  $n=6$ , paired Student's  $t$ -test). **(L)** The current amplitude induced by 5 mM ATP in the external solution with low divalent cation ( $n=8$ ) was greater than that in the normal external solution ( $n=13$ ). **(M–O)** Immunofluorescence staining showed P2X7R **(M)**, green) in mouse peritoneal mast cells, and the nucleus was stained with DAPI **(N)**, blue) (Scale bar is 50  $\mu$ m).

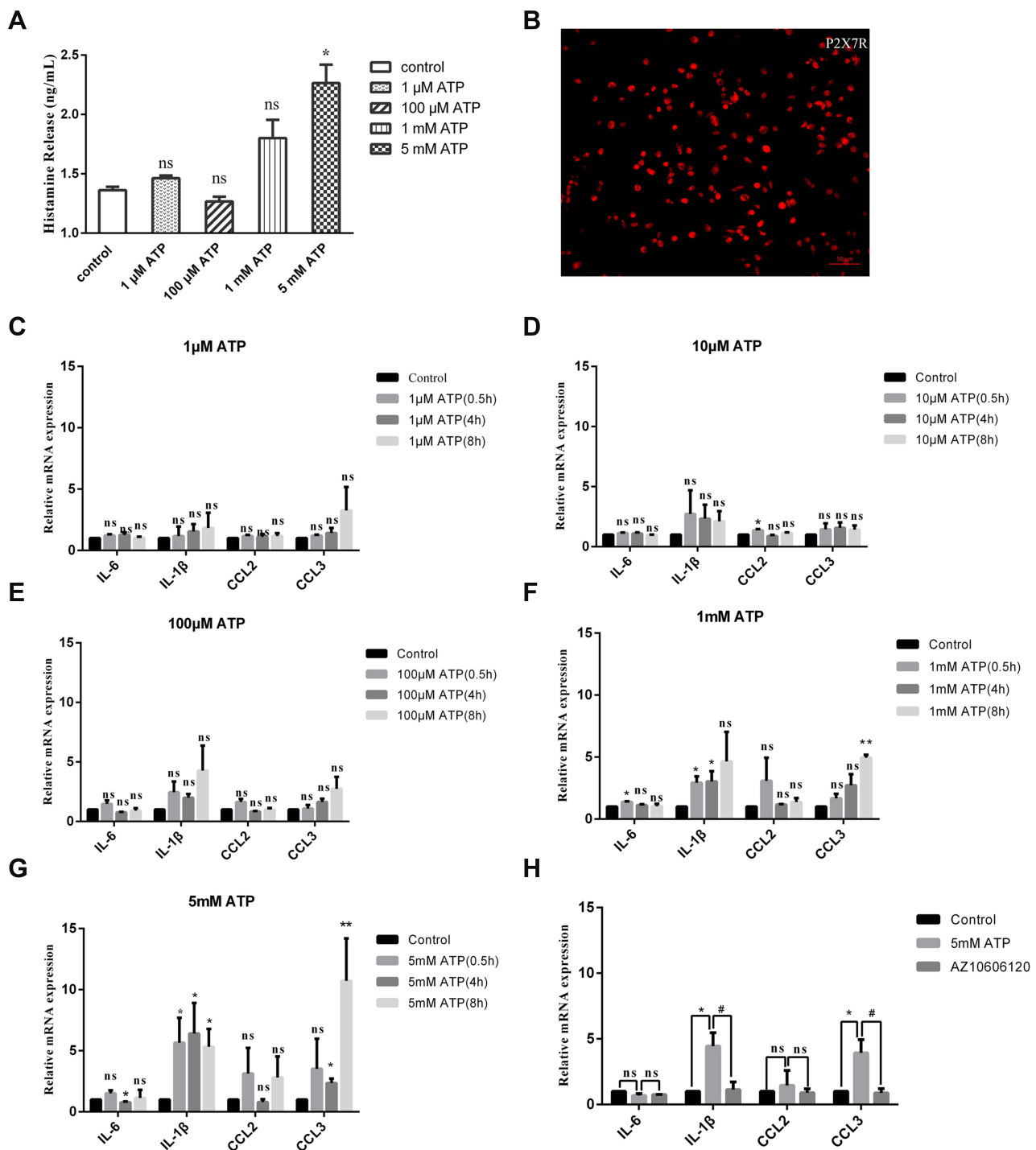


**Figure 4** Effects of extracellular ATP at different concentrations on the synthesis and release of cytokines in mast cells. **(A)** High concentrations of ATP induced significantly increased histamine release from mouse peritoneal mast cells (\* $p < 0.05$ , control vs 5 mM ATP, one-way ANOVA analysis followed by Dunnett's multiple comparisons test). **(B)** Immunofluorescence staining exhibited P2X7R (red) in P815 cells, scale bar was 50 μm. **(C–E)** There was no significant changes in the expression of IL-6, IL-1β, CCL2 and CCL3 in P815 cells induced by 1 μM ATP, 10 μM ATP or 100 μM ATP, respectively. **(F)** The expression of IL-6, IL-1β and CCL3 was up-regulated induced by 1 mM ATP in P815 cells (\* $p < 0.05$ , \*\* $p < 0.01$ , control vs 1 mM ATP, one-way ANOVA analysis followed by Dunn's multiple comparisons test). **(G)** The expression of IL-1β and CCL3 was up-regulated induced by 5 mM ATP in P815 cells (\* $p < 0.05$ , \*\* $p < 0.01$ , control vs 5 mM ATP, one-way ANOVA analysis followed by Dunn's multiple comparisons test). **(H)** The up-regulation of IL-1β and CCL3 expression caused by 5 mM ATP in P815 cells was blocked by specific P2X7R antagonist AZ10606120. (\* $p < 0.05$ , control vs 5 mM ATP; # $p < 0.05$ , 5 mM ATP vs 5 μM AZI0606120, one-way ANOVA analysis followed by Tukey's multiple comparisons test).

pain induced by high concentrations of ATP. In order to prove this hypothesis, we utilized the mast cell-deficient Kit (W-sh) Sash mutant mice and the P2X7R antagonist, AZ10606120. First, results showed that high concentrations of ATP (100 mM, 10  $\mu$ L, PH was 7.32, Intradermal injection) could induce inflammation pain, including paw swelling (Figure 5A), inflammatory cells infiltration (Figure 5B), increased paw thickness (Figure 5C), mast cells degranulation (Figure 5D), and mechanical hyperalgesia (Figure 5E). As we expected, mast cell-deficient mice could alleviate ATP-induced inflammation pain (Figure 5A–E). As shown in Figures 5F, 1 h after ATP administration, the mRNA expression levels of IL-6, IL-1 $\beta$ , CCL2 and CCL3 in C57/BL mice were significantly up-regulated. Compared with C57/BL mice, Sash mice alleviated the upregulation of IL-1 $\beta$  and CCL3 (Figure 5F). At the same time, we also investigated the role of P2X7R in ATP-induced inflammatory pain. Results showed that AZ10606120 (2 mg/kg, ip, pre-administration 1h) could significantly reduce the mechanical hypersensitivity (Figure 5H). As shown in Figure 5G, the infiltration of mast cells expressing P2X7R was significantly increased, which could be inhibited by Z10606120. Correspondingly, the upregulation of inflammatory factors such as IL-6 and CCL3 could also be blocked by AZ10606120 (Figure 5I).

## Salicylic Acid and Aspirin Inhibited the Activation of P2X7R in Mast Cells

P2X7R is an appealing target for anti-inflammatory therapy, so we used P2X7R as a target to screen for several anti-inflammatory monomers that can inhibit its activity. Results showed that Matrine, Higenamine, Dictamine, Prim-O-glucosylcimifugin, Liquiritin, Menthol, Ferulic Acid, 3-Hydroxy-4-methoxycinnamic acid, Isoginkgetin, Vanillic acid, Luteolin, Isoliquiritigenin or Aloeemodin had no inhibitory effect on the current evoked by 5 mM ATP (Supplementary Table 1). Interestingly, as shown in Figure 6A, we found that SA and ASA could inhibit the inward current induced by 5 mM ATP. Compared with the first ATP-induced current amplitude, 300  $\mu$ M, 500  $\mu$ M, or 1 mM SA slightly inhibited the second ATP-induced current amplitude (Figure 6B–D, n=21, n=14, and n=16, respectively). Notably, the current induced by 5 mM ATP had a “run-up” tendency, indicating that the current growth rate should be analyzed. Data showed that the current growth rate induced by 5 mM ATP was significantly inhibited by

SA as Figure 6E shown. 500  $\mu$ M or 1 mM ASA could also inhibit the current amplitude induced by 5 mM ATP (Figure 6F–H, n=8 and n=20 respectively). The current growth rate was significantly inhibited by 300  $\mu$ M, 500  $\mu$ M or 1 mM ASA (Figure 6I). The results of intracellular Ca<sup>2+</sup> concentration assay showed that 300  $\mu$ M SA or 1 mM ASA could also inhibit calcium influx induced by 5 mM ATP (Supplementary Figure S5). To further clarify the relationship between SA or ASA and P2X7R, the P2X7R agonist BzATP was used. Results showed that 300  $\mu$ M SA (n=18) or 300  $\mu$ M ASA (n=7) significantly inhibited the current growth rate (Figure 6J) and the calcium influx (Supplementary Figure S6) evoked by BzATP. In addition, we also found that the up-regulation of P2X7R expression could also be blocked by 500  $\mu$ M SA or 1 mM ASA (Figure 6K). As we expected, 500  $\mu$ M SA or 1 mM ASA also inhibited the up-regulation of IL-1 $\beta$  and CCL3 expression (Figure 6L), and the release of IL-1 $\beta$  and CCL3 was inhibited slightly by SA or ASA (Supplementary Figure S7).

## P2X7R in Mast Cells is a Potential Target for Salicylic Acid and Aspirin Analgesia

The previous results indicated that SA or ASA could inhibit the activity of P2X7R in mast cells, we speculated that SA or ASA might relieve inflammation pain through P2X7R. Therefore, we explored the effects of SA or ASA on the inflammation pain induced by high concentrations of ATP. Results showed that SA (50 mg/kg, ig, pretreated 1h) or ASA (50 mg/kg, ig, pretreated 1h) could relieve the mechanical hypersensitivity induced by 100 mM ATP (Figure 7B). As shown in Figure 7A, the infiltration of mast cells expressing P2X7R was significantly increased, which could be inhibited by SA or ASA. In addition, the upregulation of inflammatory factors expression including IL-6, IL-1 $\beta$  and CCL3 could also be blocked by SA or ASA (Figure 7C).

## GDP Binding Region is Critical for the Combination of Salicylic Acid and Aspirin with P2X7R

Our results suggested that the analgesic effects of SA and ASA also be achieved by inhibiting P2X7R. Next, we wondered if SA or ASA had a direct effect on P2X7R. To uncover this, we used Discovery Studio software to perform molecular docking analysis on the interaction between SA or ASA and P2X7R (Figure 8). Results showed that SA (Figure 8G–L) and its derivative ASA

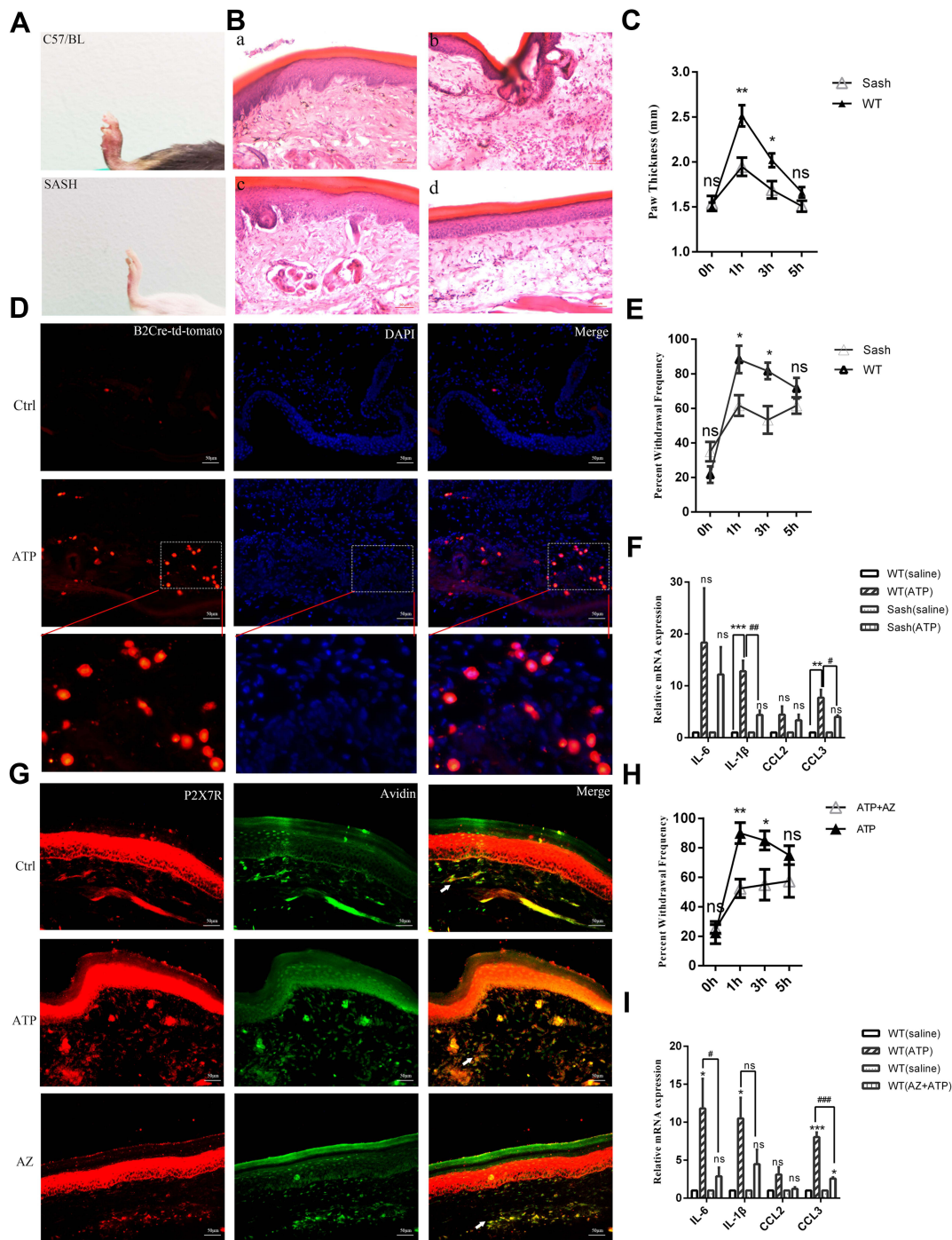


**Figure 5** Mast cell deficient and AZ10606120 alleviated high concentrations of ATP-induced inflammation pain. **(A)** Compared with C57/BL mice, Sash mice alleviated the paw swelling. **(B)** Compared with the C57/BL mice, the infiltration of inflammatory cells in Sash mice was significantly reduced. (a-b, HE staining of saline and ATP groups in C57/BL mice; c-d, HE staining of saline and ATP groups in Sash mice, 250X). **(C)** Compared with C57BL mice, Sash mice significantly reduced paw thickening (\* $p < 0.05$ , \*\* $p < 0.01$ , WT group vs Sash group,  $n=8$  and 6 respectively). **(D)** High concentrations of ATP induced mast cells degranulation (The construction of Mrgprb2-Cre tdT +mice was to integrate the fluorescent protein of Td/Tomato into the promoter of MrgprB2, red represented mast cells, and the small red granules around mast cells represented degranulation). **(E)** Sash mice alleviated the mechanical hyperalgesia by high concentrations of ATP (\* $p < 0.05$ , WT group vs Sash group,  $n=8$  and 6 respectively). **(F)** Mast cell deficient attenuated the upregulation of IL-1 $\beta$  and CCL3 (\*\* $p < 0.01$ , \*\*\* $p < 0.001$ , saline group vs ATP group, # $p < 0.05$ , ## $p < 0.01$ , WT (ATP) group vs Sash (ATP) group). **(G)** The infiltration of mast cells expressing P2X7R was significantly increased, which could be inhibited by Z10606120. **(H)** AZ10606120 significantly relieved the mechanical hyperalgesia. (\* $p < 0.05$ , \*\* $p < 0.01$ , ATP group vs ATP+AZ10606120 group). **(I)** AZ10606120 attenuated the up-regulation of IL-6 and CCL3 (\* $p < 0.05$ , \*\*\* $p < 0.001$ , saline group vs ATP group, # $p < 0.05$ , ### $p < 0.001$ , WT (ATP) group vs WT (AZ+ATP) group). (Statistical analysis of the results was performed one-way ANOVA analysis followed by Dunnett's multiple comparisons test or Tukey's multiple comparisons test).

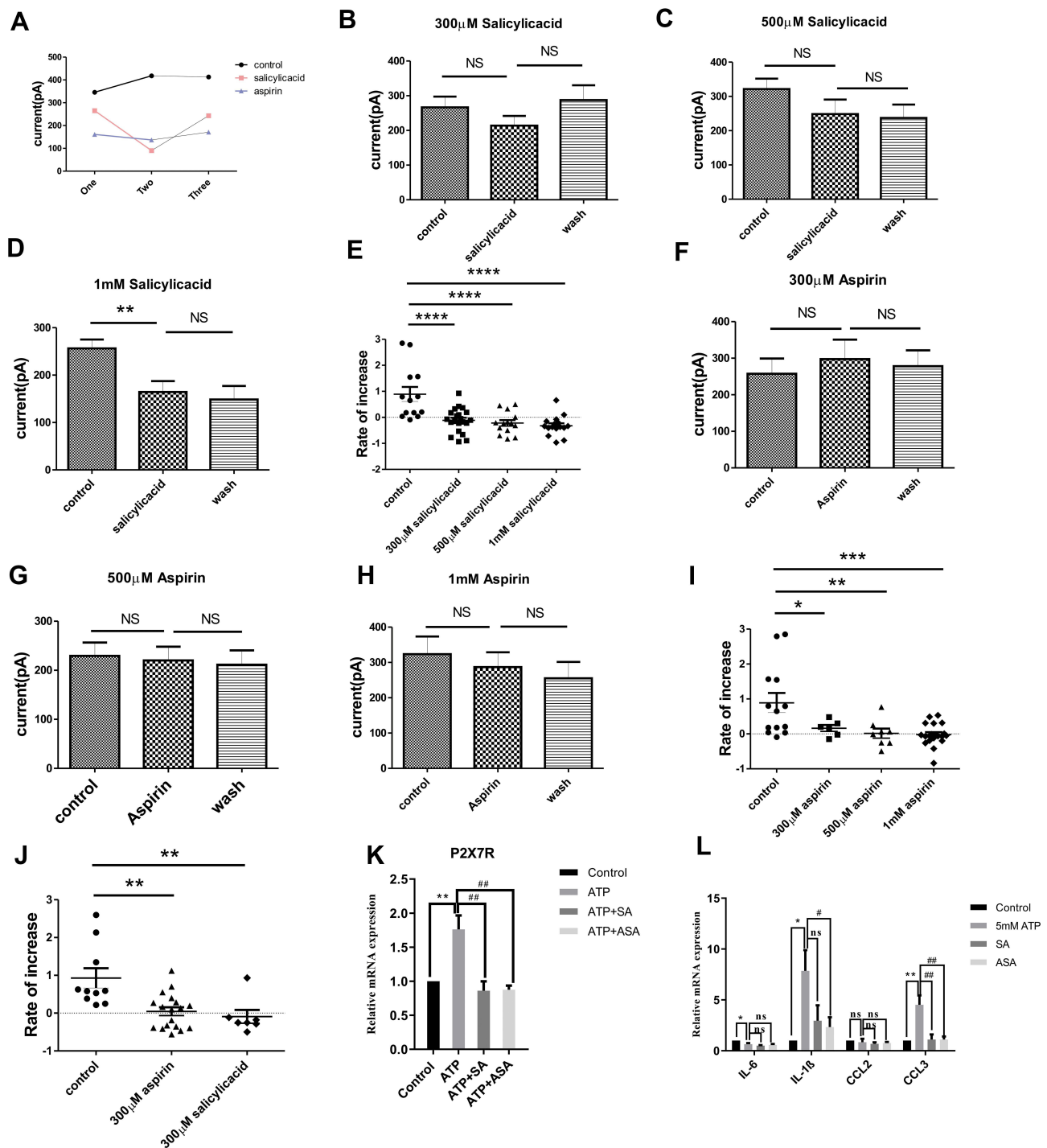


**Figure 6** The effects of SA and ASA on the activation of P2X7R in mast cells. **(A)** Schematic diagram of the effect of SA and ASA on 5 mM ATP-induced current. **(B)** Compared with the first ATP-induced current amplitude, 300 μM SA had a slight inhibitory effect on the second ATP-induced current amplitude. **(C)** Compared with the first ATP-induced current amplitude, 500 μM SA slightly inhibited the second ATP-induced current amplitude. **(D)** Compared with the first ATP-induced current amplitude, 1 mM SA significantly inhibited the second ATP-induced current amplitude (\*\* $p < 0.01$ , control vs 1 mM SA). **(E)** The current growth rate was significantly inhibited by different concentrations of SA (\*\*\*\* $p < 0.0001$ , control vs 300 μM SA, 500 μM SA or 1 mM SA). **(F–H)** Compared with the first ATP-induced current amplitude, 500 μM **(G)** or 1 mM ASA **(H)** slightly inhibited the second ATP-induced current amplitude. **(I)** The current growth rate was significantly inhibited by different concentrations of ASA (\* $p < 0.05$ , control vs 300 μM ASA; \*\* $p < 0.01$ , control vs 500 μM ASA; \*\*\*\* $p < 0.0001$ , control vs 1 mM ASA). **(J)** The current growth rate evoked by BzATP was significantly inhibited by 300 μM SA or 300 μM ASA (\*\* $p < 0.01$ , control vs 300 μM SA or 300 μM ASA). **(K)** The up-regulation of P2X7R expression induced by 5 mM ATP was blocked by 500 μM SA or 1 mM ASA (\*\* $p < 0.01$ , control vs ATP, ## $p < 0.01$ , ATP vs ATP+SA or ATP+ASA). **(L)** SA or ASA attenuated the up-regulation of IL-1β and CCL3 expression (\* $p < 0.05$ , \*\* $p < 0.01$ , control vs ATP, # $p < 0.05$ , ## $p < 0.01$ , ATP vs SA or ASA). (Statistical analysis of the results was performed one-way ANOVA analysis followed by Dunnett's multiple comparisons test or Tukey's multiple comparisons test).

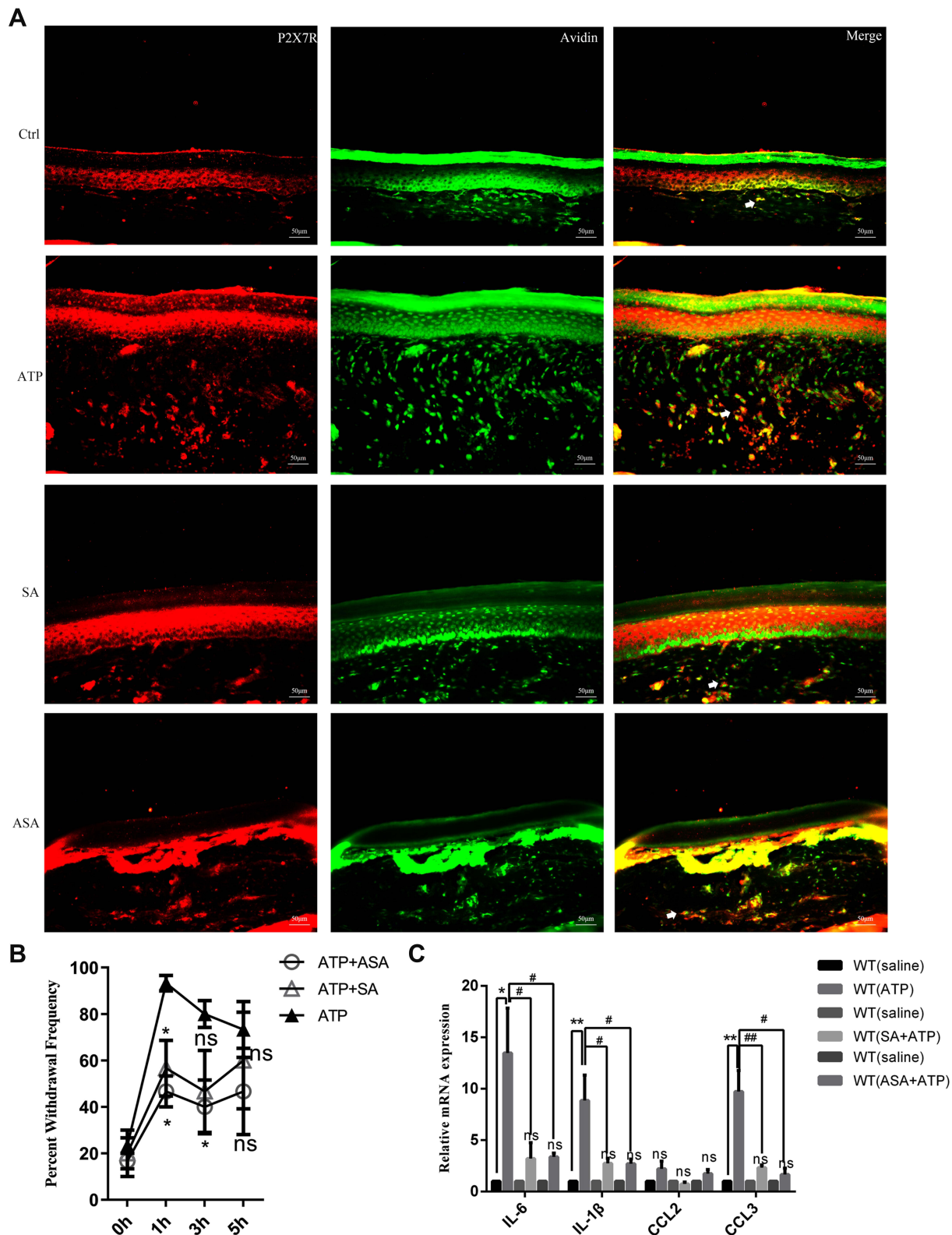


**Figure 7** The effects of SA or ASA on the inflammation pain through P2X7R. **(A)** The infiltration of mast cells expressing P2X7R was significantly increased induced by high concentrations of ATP, which could be inhibited by SA or ASA. **(B)** SA or ASA relieve the mechanical hypersensitivity induced by high concentrations of ATP (\* $p < 0.05$ , ATP vs ATP+SA or ATP+ASA). **(C)** SA or ASA attenuated the up-regulation of inflammatory factors expression (\* $p < 0.05$ , \*\* $p < 0.01$ , saline group vs ATP group, # $p < 0.05$ , ## $p < 0.01$ , WT (ATP) group vs WT (SA+ATP) or WT (ASA+ATP) group). (Statistical analysis of the results was performed one-way ANOVA analysis followed by Dunnett's multiple comparisons test or Tukey's multiple comparisons test).

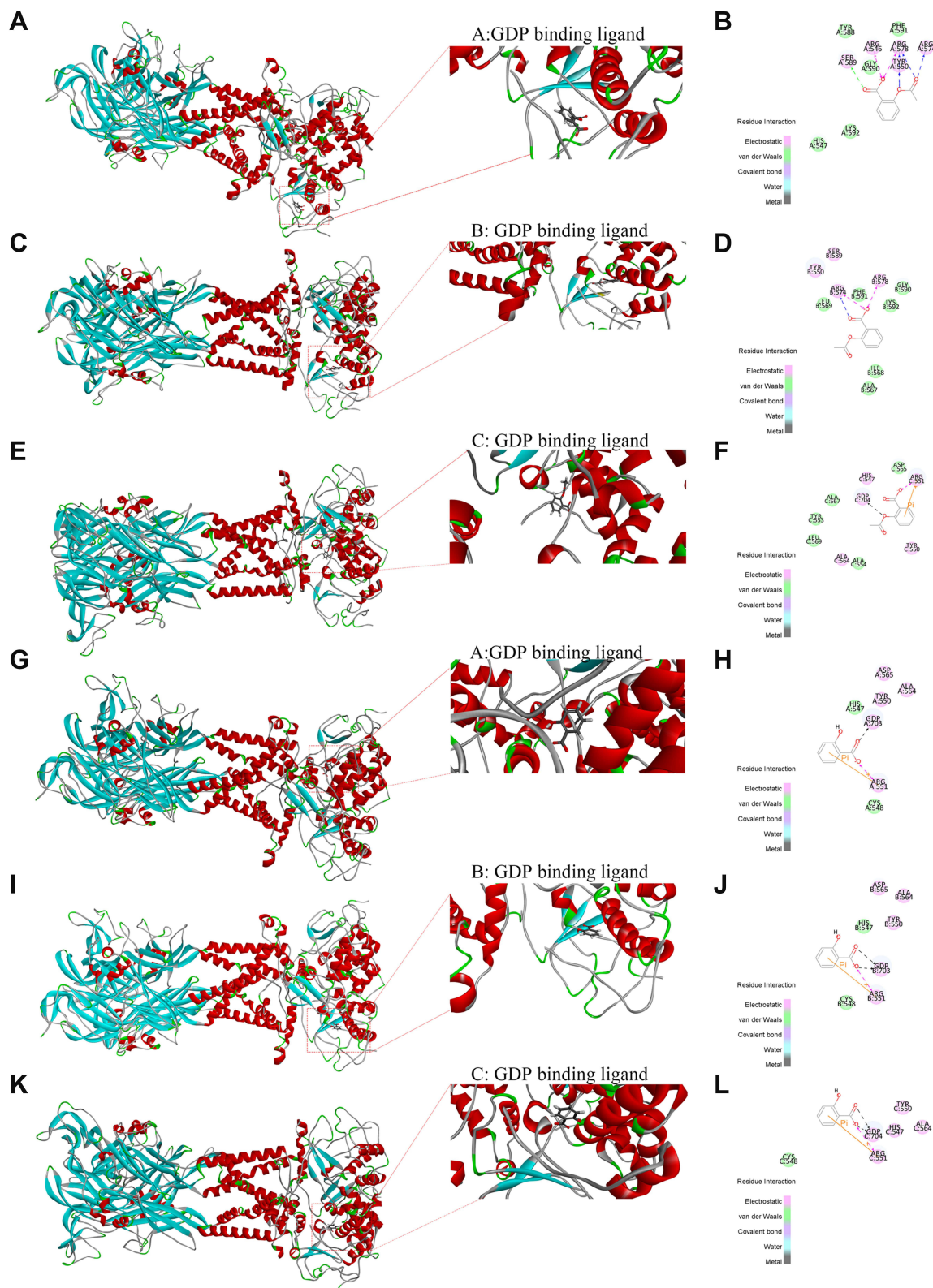


**Figure 8** Molecular docking map of compounds with P2X7R. (A and B) Docking result of ASA with the (A) GDP703 ligand of P2X7R. (C and D) Docking result of ASA with the (B) GDP703 ligand of P2X7R. (E and F) Docking result of ASA with the (C) GDP704 ligand of P2X7R. (G and H) Docking result of SA with the (A) GDP703 ligand of P2X7R. (I and J) Docking result of SA with the (B) GDP703 ligand of P2X7R. (K and L) Docking result of SA with the (C) GDP704 ligand of P2X7R.

(Figure 8A–F) had affinity with the GDP-binding region of P2X7R, including A: GDP 703, B: GDP703 and C: GDP704 ligands. Among them, ASA had the highest affinity with A: GDP 703 ligand as Figure 8A and B showed. The -COOH of aspirin formed two Electrostatic-bonds with Arg546 (R546) and Arg578 (R578) of A: GDP 703 ligand, and a van der Waals-bond with Ser589 (S589). Combined with these results, we considered that SA and ASA could inhibit P2X7R activation by directly binding the receptor, thereby reducing inflammatory pain.

## Discussion

P2X7R belongs to the family of ATP-sensitive ionotropic P2X receptors that are composed of seven homomeric receptor subtypes. P2X7R is an unusual member of the P2X receptor superfamily since it is activated by high concentrations of ATP.<sup>35</sup> P2X7R mediates NLRP3 inflammasome activation, cytokine and chemokine release, T lymphocyte survival and differentiation, transcription factor activation, and cell death.<sup>36</sup> Activation P2X7R promotes release of pro-inflammatory factors, such as IL-1 $\beta$ , IL-6, CCL2, TNF $\alpha$ , CCL3, and nitric oxide, suggesting that P2X7R is an obvious candidate to play a major and pivotal role in processes of inflammation and pain.<sup>37</sup> Inhibition of P2X7R by Brilliant BlueG (BBG) or OxATP could alleviate the inflammatory pain induced by TRPA1 agonist mustard oil.<sup>38</sup> In addition, the P2X7R antagonist OXATP also alleviates pain in arthritis induced by complete Freund's adjuvant (CFA), including a reduction of edema in the inflamed paw.<sup>39</sup> P2X7R in mast cells also has been proved to be crucial in inflammation diseases. ATP-P2X7R-mediated mast cell activation induces the recruitment of neutrophils by inflammatory cytokines, chemokines, and leukotrienes, thereby exacerbating intestinal inflammation.<sup>24</sup> Preventive oral magnesium could ameliorate colitis by reducing the accumulation of P2X7R-expressing mast cells in the colon.<sup>40</sup> In addition to intestinal inflammation, studies have shown that ATP-driven mast cell activation by P2X7R is also a potential trigger for neuro-inflammation and pain sensitization in migraine.<sup>25</sup> Until now, the relationship between P2X7R in mast cells and inflammatory pain has not been clarified. Therefore, in current study, we explored the effect of P2X7R in mast cells on inflammatory pain, and selected P2X7R as a target to screen for some anti-inflammatory monomers that inhibited its activity.

First of all, we found that several functional P2X receptors were expressed in mouse peritoneal mast cells, including P2X1R, P2X3R, P2X4R, and P2X7R. The expression profile was similar to that of mouse bone marrow mast cells, LAD2 and human lung mast cells, which expressed P2X1R, P2X4R, and P2X7R.<sup>6</sup> Extracellular ATP could induce calcium influx in mouse peritoneal mast cells in a concentration-dependent manner. Specific P2X inhibitors results indicated that P2X1R, P2X3R, P2X4R and P2X7R were involved in the calcium influx induced by 1  $\mu$ M ATP, 10  $\mu$ M ATP, 100  $\mu$ M ATP and high concentrations of ATP such as 1 mM and 5 mM, respectively. Notably, calcium influx could not be completely blocked by specific inhibitors, suggesting that other receptors were also involved. For example, in addition to P2X4R, P2Y2R can also be stimulated by ATP at a concentration of 100  $\mu$ M.<sup>23</sup> In addition, the inward currents induced by ATP in mouse peritoneal mast cells were concentration-dependent as well. Consistent with the previous studies,<sup>6</sup> our results showed that P2X1R, P2X3R, P2X4R and P2X7R were involved in the currents induced by 1  $\mu$ M ATP, 10  $\mu$ M ATP, 100  $\mu$ M ATP and high concentrations of ATP, respectively. Furthermore, the presence of P2X7R was further confirmed by immunofluorescence. Taken together, we concluded that P2X1R, P2X3R, P2X4R and P2X7R were expressed in mouse peritoneal mast cells.

To investigate the role of P2X7R in mast cells, we explored the mediator release induced by ATP. The data showed that ATP with high concentrations could induce histamine release, which was consistent with previous report.<sup>23</sup> In addition to degranulation, the expression of IL-1 $\beta$  and CCL3 in P815 cells was up-regulated by 5 mM ATP, which could be blocked by AZ10606120. These results suggested that P2X7R was involved in mast cells degranulation and the synthesis of inflammatory mediators. Neuron-immune crosstalk plays important roles in many inflammatory diseases, we hypothesize that activation of P2X7R in mast cells could indirectly induce peripheral pain, as shown in Figure 9. Histamine plays a critical role in neurogenic inflammation and pain transmission via specific receptors in a bidirectional manner.<sup>41</sup> IL-1 $\beta$  can modulate neuronal activity directly, blocking IL-1 signaling could alleviate inflammation pain.<sup>42</sup> Furthermore, the roles of inflammatory chemokines could regulate synaptic transmission, especially CCL2/CCR2 and CCL3/CCR1 signaling.<sup>43</sup> Consistent with this hypothesis, our results also showed that P2X7R in mast cells



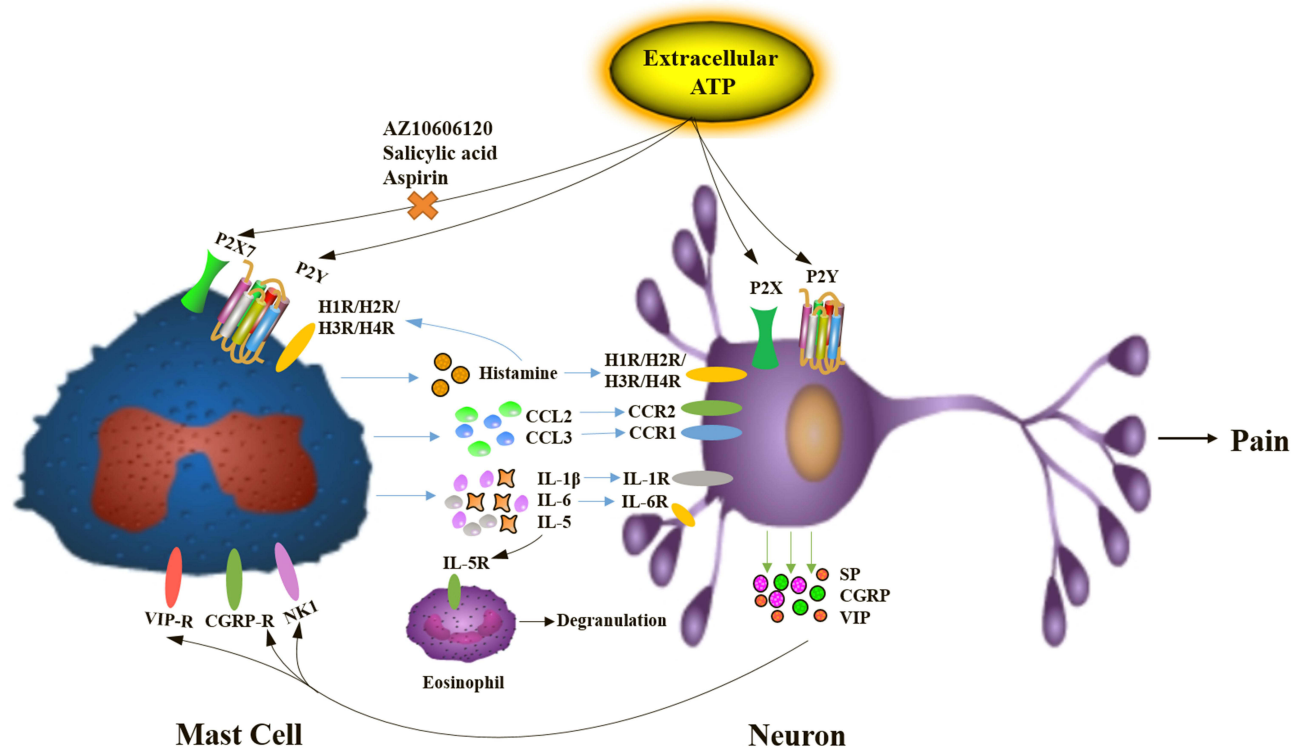


**Figure 9** The mechanism of inflammation pain induced by extracellular ATP via neuron-immune crosstalk.

participated in the inflammation pain. As shown in [Figure 5G](#), we found that P2X7R-expressing mast cells significantly increased in the inflammatory pain induced by high concentrations of ATP. AZ10606120 could alleviate this pain by inhibiting the infiltration of P2X7R-expressing mast cells.

Pain is a serious global health issue and a huge clinical challenge without available effective treatment. Therefore, the discovery of novel therapeutic alternatives with superior effectiveness and minimal adverse effects would be beneficial. P2X7R is proposed as a new drug candidate for inflammatory disorders. Therefore, we used P2X7R as a target to screen for some anti-inflammatory monomers that could inhibit its activity. Interestingly, we found that SA and ASA could inhibit the inward current and calcium influx induced by ATP with high concentrations or P2X7R agonist BZATP. Meanwhile, SA and ASA also inhibited the up-regulation of P2X7R, IL-1 $\beta$  and CCL3 expression induced by high concentrations of ATP in vitro. Moreover, we also found that SA and ASA could alleviate the inflammatory pain induced by high concentrations of ATP in vivo, which was related to reducing the recruitment of mast cells expressing P2X7R. Molecular docking results showed that SA and ASA had affinity with

the cytoplasmic GDP-binding region of P2X7R. Therefore, SA and ASA may inhibit the activity of P2X7R by binding the GDP-binding region, thereby alleviating inflammatory pain. The binding patterns and binding sites of SA and ASA on P2X7R need to be further verified.

## Conclusion

In summary, we found that mouse-derived mast cells could be activated by extracellular ATP via P2X1, P2X3, P2X4, and P2X7 receptors. Activation of P2X7R in mast cells played an important role in inflammatory pain by releasing inflammatory mediators. In addition, we also found that P2X7R might be a potential target for analgesics SA and ASA.

## Abbreviations

ATP, adenosine-triphosphate; P2X7R, P2X7 receptor; IL-1 $\beta$ , interleukin-1 $\beta$ ; IL-6, interleukin-6; CCL2, C-C motif chemokine 2; CCL3, C-C motif chemokine 3; GDP, guanosine diphosphate; MrgprB2, MAS-related GPR member B2; SCF, stem cell growth factors; SA, salicylic acid; ASA, acetylsalicylic acid.

## Acknowledgments

The authors thank Prof. Xinzhong Dong in Johns Hopkins for kindly providing the Mast cell-deficient Kit (W-sh) “Sash” mutant mice and Mrgprb2-Cre tdT +mice. The authors thank Prof. Ye Yu in China Pharmaceutical University for kindly providing the P2X3R antagonist AF-353.

## Author Contributions

All authors made a significant contribution to the work reported, whether that is in the conception, study design, execution, acquisition of data, analysis and interpretation, or in all these areas; took part in drafting, revising or critically reviewing the article; gave final approval of the version to be published; have agreed on the journal to which the article has been submitted; and agree to be accountable for all aspects of the work.

## Funding

The study was financially supported by National Natural Science Foundation of China (No. 31771163), the key project of science and technology development plan of traditional Chinese medicine in Jiangsu Province (No. ZD202001), and Innovative Project of postgraduate education in Jiangsu Province (No. 021093002404).

## Disclosure

The authors declare that they have no competing interests.

## References

- Luo J, Feng J, Liu S, et al. Molecular and cellular mechanisms that initiate pain and itch. *Cell Mol Life Sci.* 2015;72(17):3201–3223.
- Xu H, Bin NR, Sugita S. Diverse exocytic pathways for mast cell mediators. *Biochem Soc Trans.* 2018;46(2):235–247. doi:10.1042/BST20170450
- Gupta K, Harvima IT. Mast cell-neural interactions contribute to pain and itch. *Immunol Rev.* 2018;282(1):168–187.
- Kim HS, Kawakami Y, Kasakura K, et al. Recent advances in mast cell activation and regulation. *F1000Res.* 2020;9:F1000Faculty Rev–196. doi:10.12688/f1000research.22037.1
- Yu Y, Blokhuis BR, Garssen J, et al. Non-IgE mediated mast cell activation. *Eur J Pharmacol.* 2016;778:33–43. doi:10.1016/j.ejphar.2015.07.017
- Wareham K, Vial C, Wykes RC, et al. Functional evidence for the expression of P2X1, P2X4 and P2X7 receptors in human lung mast cells. *Br J Pharmacol.* 2009;157(7):1215–1224. doi:10.1111/j.1476-5381.2009.00287.x
- Jacobson KA, Muller CE. Medicinal chemistry of adenosine, P2Y and P2X receptors. *Neuropharmacology.* 2016;104:31–49. doi:10.1016/j.neuropharm.2015.12.001
- Franceschini A, Adinolfi E. P2X receptors: new players in cancer pain. *World J Biol Chem.* 2014;5(4):429–436. doi:10.4331/wjbc.v5.i4.429
- Kuan YH, Shyu BC. Nociceptive transmission and modulation via P2X receptors in central pain syndrome. *Mol Brain.* 2016;9(1):58.

- Inoue K, Tsuda M. Nociceptive signaling mediated by P2X3, P2X4 and P2X7 receptors. *Biochem Pharmacol.* 2020;29:114309.
- Tewari M, Seth P. Emerging role of P2X7 receptors in CNS health and disease. *Ageing Res Rev.* 2015;24(Pt B):328–342. doi:10.1016/j.arr.2015.10.001
- Broom DC, Matson DJ, Bradshaw E, et al. Characterization of N-(adamantan-1-ylmethyl)-5-[(3R-amino-pyrrolidin-1-yl)methyl]-2-chloro-benzamide, a P2X7 antagonist in animal models of pain and inflammation. *J Pharmacol Exp Ther.* 2008;327(3):620–633. doi:10.1124/jpet.108.141853
- McGarraughty S, Chu KL, Namovic MT, et al. P2X7-related modulation of pathological nociception in rats. *Neuroscience.* 2007;146(4):1817–1828. doi:10.1016/j.neuroscience.2007.03.035
- Chessell IP, Hatcher JP, Bountra C, et al. Disruption of the P2X7 purinoceptor gene abolishes chronic inflammatory and neuropathic pain. *Pain.* 2005;114(3):386–396. doi:10.1016/j.pain.2005.01.002
- Yang Y, Li H, Li TT, et al. Delayed activation of spinal microglia contributes to the maintenance of bone cancer pain in female Wistar rats via P2X7 receptor and IL-18. *J Neurosci.* 2015;35(20):7950–7963. doi:10.1523/JNEUROSCI.5250-14.2015
- Ferrari D, Pizzirani C, Adinolfi E, et al. The P2X7 receptor: a key player in IL-1 processing and release. *J Immunol.* 2006;176(7):3877–3883. doi:10.4049/jimmunol.176.7.3877
- Karmakar M, Katsnelson MA, DUBYAK GR, et al. Neutrophil P2X7 receptors mediate NLRP3 inflammasome-dependent IL-1beta secretion in response to ATP. *Nat Commun.* 2016;7:10555. doi:10.1038/ncomms10555
- Kataoka A, Tozaki-Saitoh H, Koga Y, et al. Activation of P2X7 receptors induces CCL3 production in microglial cells through transcription factor NFAT. *J Neurochem.* 2009;108(1):115–125. doi:10.1111/j.1471-4159.2008.05744.x
- Parzych K, Zetterqvist AV, Wright WR, et al. Differential role of pannexin-1/ATP/P2X7 axis in IL-1beta release by human monocytes. *FASEB J.* 2017;31(6):2439–2445. doi:10.1096/fj.201600256
- Shieh CH, Heinrich A, Serchov T, et al. P2X7-dependent, but differentially regulated release of IL-6, CCL2, and TNF-alpha in cultured mouse microglia. *Glia.* 2014;62(4):592–607. doi:10.1002/glia.22628
- Bulanova E, Bulfone-Paus S. P2 receptor-mediated signaling in mast cell biology. *Purinergic Signal.* 2010;6(1):3–17. doi:10.1007/s11302-009-9173-z
- Wareham KJ, Seward EP. P2X7 receptors induce degranulation in human mast cells. *Purinergic Signal.* 2016;12(2):235–246. doi:10.1007/s11302-016-9497-4
- Yoshida K, Ito M, Matsuoka I. Divergent regulatory roles of extracellular ATP in the degranulation response of mouse bone marrow-derived mast cells. *Int Immunopharmacol.* 2017;43:99–107. doi:10.1016/j.intimp.2016.12.014
- Kurashima Y, Amiya T, Nochi T, et al. Extracellular ATP mediates mast cell-dependent intestinal inflammation through P2X7 purinoceptors. *Nat Commun.* 2012;3:1034. doi:10.1038/ncomms2023
- Nurkhametova D, Kudryavtsev I, Guseynikova V, et al. Activation of P2X7 receptors in peritoneal and meningeal mast cells detected by uptake of organic dyes: possible purinergic triggers of neuroinflammation in meninges. *Front Cell Neurosci.* 2019;13:45. doi:10.3389/fncel.2019.00045
- Munir MA, Enany N, Zhang JM. Nonopioid analgesics. *Anesthesiol Clin.* 2007;25(4):761–774. doi:10.1016/j.anclin.2007.07.007
- Gordon DB. Nonopioid and adjuvant analgesics in chronic pain management: strategies for effective use. *Nurs Clin North Am.* 2003;38(3):447–464. doi:10.1016/S0029-6465(02)00095-6
- Vane JR, Botting RM. The mechanism of action of aspirin. *Thromb Res.* 2003;110(5–6):255–258. doi:10.1016/S0049-3848(03)00379-7

29. Kim HM, Shin HY, Choo YK, et al. Inhibition of mast cell-dependent anaphylaxis by sodium salicylate. *Immunology*. 1999;96(4):551–556. doi:10.1046/j.1365-2567.1999.00729.x
30. Steinke JW, Payne SC, Borish L. Eosinophils and mast cells in aspirin-exacerbated respiratory disease. *Immunol Allergy Clin North Am*. 2016;36(4):719–734. doi:10.1016/j.iac.2016.06.008
31. Steinke JW, Negri J, Liu L, et al. Aspirin activation of eosinophils and mast cells: implications in the pathogenesis of aspirin-exacerbated respiratory disease. *J Immunol*. 2014;193(1):41–47. doi:10.4049/jimmunol.1301753
32. Mortaz E, Redegeld FA, Nijkamp FP, et al. Dual effects of acetylsalicylic acid on mast cell degranulation, expression of cyclooxygenase-2 and release of pro-inflammatory cytokines. *Biochem Pharmacol*. 2005;69(7):1049–1057. doi:10.1016/j.bcp.2004.12.018
33. McNeil BD, Pundir P, Meeker S, et al. Identification of a mast-cell-specific receptor crucial for pseudo-allergic drug reactions. *Nature*. 2015;519(7542):237–241. doi:10.1038/nature14022
34. North RA. Molecular physiology of P2X receptors. *Physiol Rev*. 2002;82(4):1013–1067. doi:10.1152/physrev.00015.2002
35. Jacobson KA, Jarvis MF, Williams M. Purine and pyrimidine (P2) receptors as drug targets. *J Med Chem*. 2002;45:4057–4093. doi:10.1021/jm020046y
36. Di Virgilio F, Dal Ben D, Sarti AC, et al. The P2X7 receptor in infection and inflammation. *Immunity*. 2017;47(1):15–31. doi:10.1016/j.immuni.2017.06.020
37. Hughes JP, Hatcher JP, Chessell IP. The role of P2X<sub>7</sub> in pain and inflammation. *Purinergic Signal*. 2007;3(1–2):163–169. doi:10.1007/s11302-006-9031-1
38. Itoh K, Chiang C, Li Z, et al. Central sensitization of nociceptive neurons in rat medullary dorsal horn involves purinergic P2X<sub>7</sub> receptors. *Neuroscience*. 2011;192:721–731. doi:10.1016/j.neuroscience.2011.06.083
39. Dell’Antonio G, Quattrini A, Cin ED, et al. Relief of inflammatory pain in rats by local use of the selective P2X<sub>7</sub> ATP receptor inhibitor, oxidized ATP. *Arthritis Rheum*. 2002;46:3378–3385. doi:10.1002/art.10678
40. Ohbori K, Fujiwara M, Ohishi A, et al. Prophylactic oral administration of magnesium ameliorates dextran sulfate sodium-induced colitis in mice through a decrease of colonic accumulation of P2X<sub>7</sub> receptor-expressing mast cells. *Biol Pharm Bull*. 2017;40(7):1071–1077. doi:10.1248/bpb.b17-00143
41. Rosa AC, Fantozzi R. The role of histamine in neurogenic inflammation. *Br J Pharmacol*. 2013;170(1):38–45. doi:10.1111/bph.12266
42. White FA, Bhangoo SK, Miller RJ. Chemokines: integrators of pain and inflammation. *Nat Rev Drug Discov*. 2005;4(10):834–844. doi:10.1038/nrd1852
43. Ren K, Torres R. Role of interleukin-1beta during pain and inflammation. *Brain Res Rev*. 2009;60(1):57–64. doi:10.1016/j.brainresrev.2008.12.020

## Journal of Inflammation Research

Dovepress

### Publish your work in this journal

The Journal of Inflammation Research is an international, peer-reviewed open-access journal that welcomes laboratory and clinical findings on the molecular basis, cell biology and pharmacology of inflammation including original research, reviews, symposium reports, hypothesis formation and commentaries on: acute/chronic inflammation; mediators of inflammation; cellular processes; molecular

mechanisms; pharmacology and novel anti-inflammatory drugs; clinical conditions involving inflammation. The manuscript management system is completely online and includes a very quick and fair peer-review system. Visit <http://www.dovepress.com/testimonials.php> to read real quotes from published authors.

Submit your manuscript here: <https://www.dovepress.com/journal-of-inflammation-research-journal>